doi:10.1093/jmcb/mjv005
Published online January 20, 2015

Article

mTOR signaling promotes stem cell activation via counterbalancing BMP-mediated suppression during hair regeneration

Zhili Deng[1,2,†], Xiaohua Lei[1,†], Xudong Zhang[1,2], Huishan Zhang[1,2], Shuang Liu[1], Qi Chen[1], Huimin Hu[1], Xinyue Wang[1,2], Lina Ning[1], Yujing Cao[1], Tongbiao Zhao[1], Jiaxi Zhou[3], Ting Chen[4], and Enkui Duan[1,*]

[1] State Key Laboratory of Reproductive Biology, Institute of Zoology, Chinese Academy of Sciences, Beijing 100101, China
[2] University of Chinese Academy of Sciences, Beijing 100190, China
[3] State Key Laboratory of Experimental Hematology, Institute of Hematology & Blood Diseases Hospital, Chinese Academy of Medical Sciences & Peking Union Medical College, Tianjin 300020, China
[4] National Institute of Biological Sciences, Beijing 102206, China
[†] These authors contributed equally to this work.
[*] Correspondence to: Enkui Duan, E-mail: duane@ioz.ac.cn

Hair follicles (HFs) undergo cycles of degeneration (catagen), rest (telogen), and regeneration (anagen) phases. Anagen begins when the hair follicle stem cells (HFSCs) obtain sufficient activation cues to overcome suppressive signals, mainly the BMP pathway, from their niche cells. Here, we unveil that mTOR complex 1 (mTORC1) signaling is activated in HFSCs, which coincides with the HFSC activation at the telogen-to-anagen transition. By using both an inducible conditional gene targeting strategy and a pharmacological inhibition method to ablate or inhibit mTOR signaling in adult skin epithelium before anagen initiation, we demonstrate that HFs that cannot respond to mTOR signaling display significantly delayed HFSC activation and extended telogen. Unexpectedly, BMP signaling activity is dramatically prolonged in mTOR signaling-deficient HFs. Through both gain- and loss-of-function studies *in vitro*, we show that mTORC1 signaling negatively affects BMP signaling, which serves as a main mechanism whereby mTORC1 signaling facilitates HFSC activation. Indeed, *in vivo* suppression of BMP by its antagonist Noggin rescues the HFSC activation defect in mTORC1-null skin. Our findings reveal a critical role for mTOR signaling in regulating stem cell activation through counterbalancing BMP-mediated repression during hair regeneration.

Keywords: mTOR, skin, hair follicle, stem cells, BMP

Introduction

Adult stem cells (SCs) are essential for tissue homeostasis and regeneration. The hair follicles (HFs) provide an elegant model for studying the balance between quiescence and activation of stem cells responsible for these processes. Hair follicles repeatedly cycle through bouts of degeneration (catagen), rest (telogen), and growth (anagen) throughout adult life (Millar, 2002; Schneider et al., 2009). This hair cycle is based on the ability of hair follicle stem cells (HFSCs), a type of slow-cycling, label-retaining cells residing in a niche called the bulge, to transiently exit their quiescent status to fuel the growth phase (Cotsarelis et al., 1990; Tumbar et al., 2004; Kandyba et al., 2013). During the telogen-to-anagen transition, hair germ (HG) cells, a HFSC-derived small cell cluster between the bulge and dermal papilla (DP), are primed to launch HF regeneration responding to DP signals (Greco et al., 2009).

At different phases of the hair cycle, HFSCs receive activating or suppressive cues from the surrounding niche to become proliferative or remain quiescent (Plikus, 2012). It has been shown that fine tuning of two signaling pathways, namely Wnt/β-catenin and bone morphogenetic protein (BMP) signaling, plays key roles in driving HFs from telogen to anagen. The activating Wnt/β-catenin signaling is believed to facilitate the stem cell activation and anagen initiation (Andl et al., 2002; Zhang et al., 2008; Enshell-Seijffers et al., 2010; Rabbani et al., 2011; Plikus, 2012). Particularly, inactivation of β-catenin in adult HFs prevents the activation of HFSCs and restrains the entry into anagen, while overexpression of β-catenin results in the precocious activation of HFSCs and premature anagen onset (Lowry et al., 2005).

In contrast to Wnt-activating signals, BMP signaling plays an inhibitory role in the activation of HFSCs (Zhang et al., 2006; Plikus et al., 2008). During telogen, active BMP signaling is critical for

Received July 11, 2014. Revised October 28, 2014. Accepted October 30, 2014.

maintaining HFSCs in a relatively quiescent state (Horsley et al., 2008; Plikus et al., 2008). Ablation of the BMP receptor Bmpr1a in adult hair follicles leads to precocious HFSC activation (Kobielak et al., 2007). Similarly, overexpression of Noggin, an extracellular BMP inhibitor, results in a shortened telogen phase and promotes HF growth (Botchkarev et al., 2001). Conversely, overexpression of BMP leads to delayed HFSC activation and prolonged telogen phase, and thus retards the HF growth (Botchkarev et al., 2001; Plikus et al., 2008). In addition, it has recently been shown that TGFβ2 signaling also plays a crucial role in the telogen-to-anagen transition in HFSC activation (Oshimori and Fuchs, 2012).

Despite the wealth of knowledge regarding these key pathways, little is known about the role of nutrient and energy effectors in regulating HFSCs. The mammalian target of rapamycin (mTOR), a serine/threonine protein kinase, is a key component of a signaling pathway that integrates a myriad of signals, ranging from nutrient availability and energy status to cellular stressors and growth factors, to regulate organism growth and homeostasis in mammals (Laplante and Sabatini, 2012). mTOR interacts with several other proteins to form two distinct complexes, namely rapamycin-sensitive mTOR complex 1 (mTORC1) and rapamycin-insensitive mTOR complex 2 (mTORC2), which are functionally conserved in eukaryotes (Gan and DePinho, 2009; Russell et al., 2011). Previous studies have demonstrated that mTORC1 signaling is essential for the proliferation of some stem cells (Javier et al., 1997; Hay and Sonenberg, 2004; Murakami et al., 2004; Ryu and Han, 2011). Notably, mTORC1 signaling pathway also plays a critical role in regulating the quiescence of hematopoietic stem cells (Gan and DePinho, 2009; Gan et al., 2010) and determining proliferation versus quiescence in the adult forebrain neural stem cell niche (Paliouras et al., 2012). Although mTOR signaling is vital for stem cell proliferation and quiescence, its potential roles for HFSCs and hair regeneration remain largely undefined.

Here, we focus on addressing the role of mTOR signaling in HFSC activation during hair regeneration. We demonstrate that mTORC1 signaling is activated in HFSCs during the telogen-to-anagen transition. By employing both an inducible conditional gene targeting strategy and a pharmacological inhibition method to ablate or inhibit mTOR signaling in adult HFs before anagen onset, we show that HFs deficient in this signaling display a remarkable delay in HFSC activation and dramatically prolonged telogen phase. Through both gain- and loss-of-function studies, we find that mTORC1 signaling negatively affects BMP signaling in HFSCs. Furthermore, exogenously supplied BMP antagonist Noggin can rescue the delayed HFSC activation and prolonged telogen in mTORC1-deficient mice. Taken together, these findings shed significant new light on how HFSC activation is orchestrated by mTORC1 signaling pathway during hair regeneration.

Results

mTOR signaling is activated in stem cells during the telogen-to-anagen transition

To define the roles of mTOR signaling in HF regeneration, we first examined the expression of pS6, the phosphorylated form of the mTORC1 downstream molecule S6 (Wendel et al., 2004), at distinct hair cycle stages determined as previously described (Muller-Rover et al., 2001; Greco et al., 2009; Oshimori and Fuchs, 2012). After hair morphogenesis, the first signs of active mTORC1 signaling occurred at telogen, when *cytoplasmic* localization of pS6 was detected in HG cells near the DP. With anagen initiating, *S6 phosphorylation* also appeared in HFSCs marked by CD34 at the base of the bulge (Figure 1A). However, when hair follicles entered full anagen, pS6 was turned off in HFSCs (Supplementary Figure S1A).

When the first anagen and second catagen ended, HFs reached the second telogen that was sustained for ~1 month in WT/control mice. The activity of pS6 was extremely weak during early and mid-telogen. Then pS6 reemerged in HG (marked by P-cadherin) and lower bulge cells when telogen ended (Figure 1B). Particularly, pS6 appeared several days before HG cells displayed proliferative activity, and this expression pattern of pS6 was consistent with the proliferation of HFSCs in HG and bulge (Figure 1C). In the meantime, we also examined the expression of p-Akt (Ser473), the phosphorylated form of Akt directly activated by mTORC2 through phosphorylating its hydrophobic motif (Ser473) (Sarbassov et al., 2005). By immunostaining, we showed that mTORC2 signaling was activated in hair follicles, mainly in the inner root sheath (IRS) rather than in the outer root sheath (ORS) including bulge and HG, during the telogen-to-anagen transition (Supplementary Figure S1C), which suggested that mTORC2 may not be involved in the telogen-to-anagen transition. Thus, we focused on the mTORC1 signaling.

We confirmed the phosphorylation pattern of S6 by performing immunoblot analysis on proteins from isolated bulge cells of different hair cycle stages. We isolated 1st anagen (P24, 24 days after birth), 2nd telogen (P56), and 2nd anagen (P82) bulge cells by FACS using the surface markers α6-integrin and CD34 as previously described (Blanpain et al., 2004). Immunoblot analysis showed that pS6 was relatively highly expressed in anagen bulge cells rather than telogen bulge cells (Figure 1D and Supplementary Figure S1B), which was consistent with our immunostaining results *in vivo* (Figure 1A–C).

To further examine mTORC1 signaling, we depilated the mid-dorsal hair coat of 8-week-old mice to provide a proliferative stimulus and to synchronize the anagen entry of hair follicles (Muller-Rover et al., 2001; Chen et al., 2012). By pS6 immunostaining, we found that mTORC1 signaling was unexpectedly activated in DP ~2 h after depilation. With anagen initiation, pS6 waned in DP, but arose in HG and bulge cells (Figure 1E). Similar to the spontaneous hair cycle, the appearance of pS6 coincided with the activation of stem cells in HG/bulge (Figure 1F). Overall, the activation of mTORC1 rather than mTORC2 signaling in HG and bulge coincides with stem cell activation during hair regeneration.

Genetic and pharmacological ablation of mTOR signaling results in prolonged telogen phase

To determine whether mTOR signaling was required for adult hair regeneration, mTOR was inducibly deleted in adult skin epithelium by crossing *mTOR(fl/fl)*-floxed mice (Risson et al., 2009) with *K14-Cre*^{TM} mice (Vasioukhin et al., 1999). Offspring from matings of

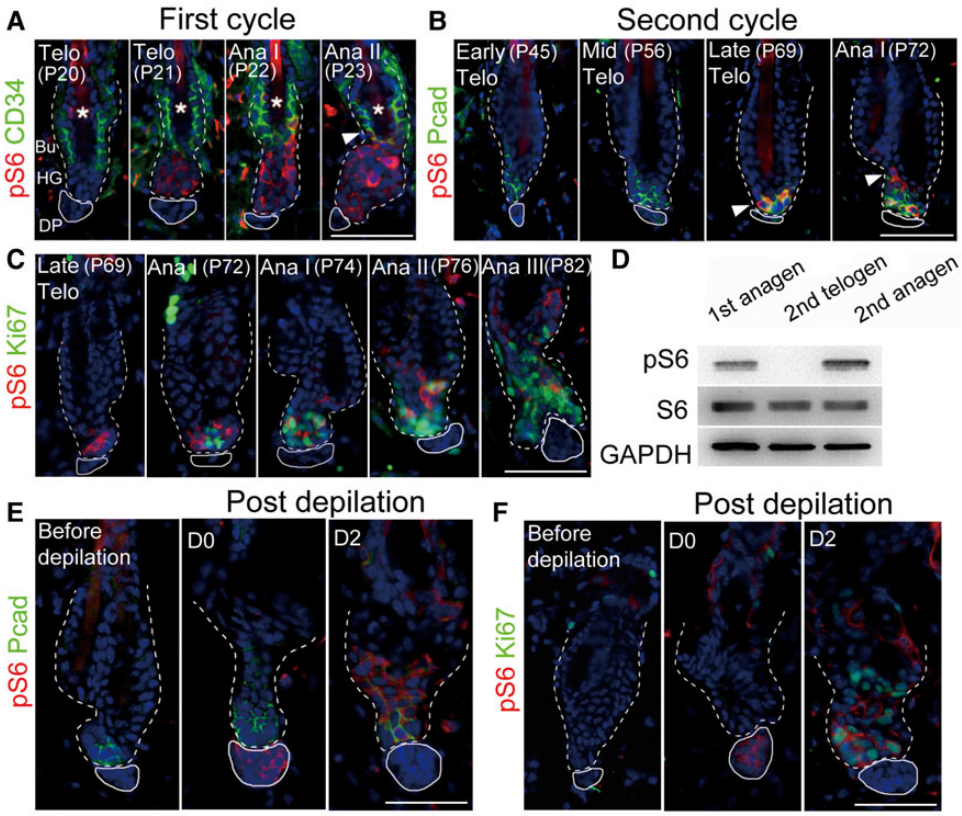

Figure 1 mTOR signaling is activated in hair follicle stem cells at the telogen-to-anagen transition during hair regeneration. (**A**) Immunostaining of pS6 in HFs during the first telogen-to-anagen transition. CD34 marks the bulge. Arrowhead indicates bulge cells that express pS6. White asterisks denote the autofluorescence (not immunostaining) on the hair shaft. Telo, telogen; Ana, anagen; P20, postnatal day 20; Bu, bulge; HG, hair germ; DP, dermal papilla. (**B**) pS6 immunostaining in HFs from the extended second telogen to the next anagen. P-cadherin (Pcad) marks the HG. White arrowheads note two distinct sites of pS6 staining, namely HG and bulge. Early Telo stands for early telogen, the initial stage of telogen, also known as refractory telogen; Mid Telo stands for mid-telogen, a period time between early telogen and late telogen; Late Telo stands for late telogen, the ending stage of telogen, also known as competent telogen (Plikus et al., 2008; Greco et al., 2009). (**C**) pS6 and Ki67 immunolocalizations in HFs upon HFSC activation. mTOR signaling is activated at the telogen-to-anagen transition. (**D**) Isolated 1st anagen (P24), 2nd telogen (P56), and 2nd anagen (P82) HFSCs through FACS were subjected to immunoblotting analysis. (**E**) Immunostaining of pS6 in HFs before depilation (P56), 0 day post depilation (D0), and 2 days post depilation (D2). (**F**) pS6 and Ki67 coemerge upon HFSC activation post depilation. DAPI staining (blue) indicates nuclear localization. Dermal–epidermal boundary is noted by dashed lines; Solid lines note the DP. Scale bar, 50 μm.

K14-Cre^{TM}/*mTOR*(*fl*/+) mice yielded litters of the expected numbers, genotype, and mendelian ratio. Tamoxifen (TM) was intraperitoneally injected to induce Cre-dependent recombination in *K14-Cre*^{TM}/*mTOR*(*fl*/*fl*) mice, which were indistinguishable from control (CON) mice including wild type (WT), *mTOR*(*fl*/+), *mTOR*(*fl*/*fl*), *K14-Cre*^{TM}/*mTOR*(*fl*/+), and *K14-Cre*^{TM}/*mTOR*(+/+). At P56, HFs had entered second mid-telogen, when both *K14-Cre*^{TM}/*mTOR*(*fl*/*fl*) (cKO) and CON HFs displayed the morphology of telogen-phase (data not shown). At this time, we shaved the mice and intraperitoneally injected with TM (Figure 2A). After 2 weeks, we validated that *mTOR* gene was efficiently targeted by anti-mTOR and anti-pS6 immunofluorescence (Figure 2B and Supplementary Figure S2A).

K14-Cre^{TM}/*mTOR*(*fl*/*fl*) mice treated with TM (cKO^{TM}), deficient in the activation of mTOR signaling in HFSCs, exhibited significantly delayed hair regrowth compared with control mice treated with TM (CON^{TM}); and in particular, by histological analysis, we found that at P100, HFs of CON^{TM} mice entered full anagen, while cKO^{TM} HFs still remained in telogen (Figure 2C).

In addition, pharmacological inhibition of mTORC1 signaling by rapamycin (RAPA) (Castilho et al., 2009) before anagen initiation in both the first and second hair cycles (Figure 2A), was also employed to investigate the role of mTORC1 signaling in hair regeneration. The effect of RAPA on repressing mTORC1 rather than mTORC2 signaling in hair follicles was verified by anti-pS6 and anti-p-Akt (Ser473) immunofluorescence, respectively (Figure 2D, E and Supplementary Figure S2B). Similar to the phenotype of cKO^{TM} mice, the hair regrowth of mice treated with RAPA was prominently retarded compared with that of mice treated with vehicle (CON); and particularly, HFs of RAPA mice were restrained in telogen when CON HFs had already entered mid-/late anagen (Figure 2F and G). To test whether the delay of hair growth in mice treated with RAPA is due to the delay of entire body maturation, we assessed the body weights of mice.

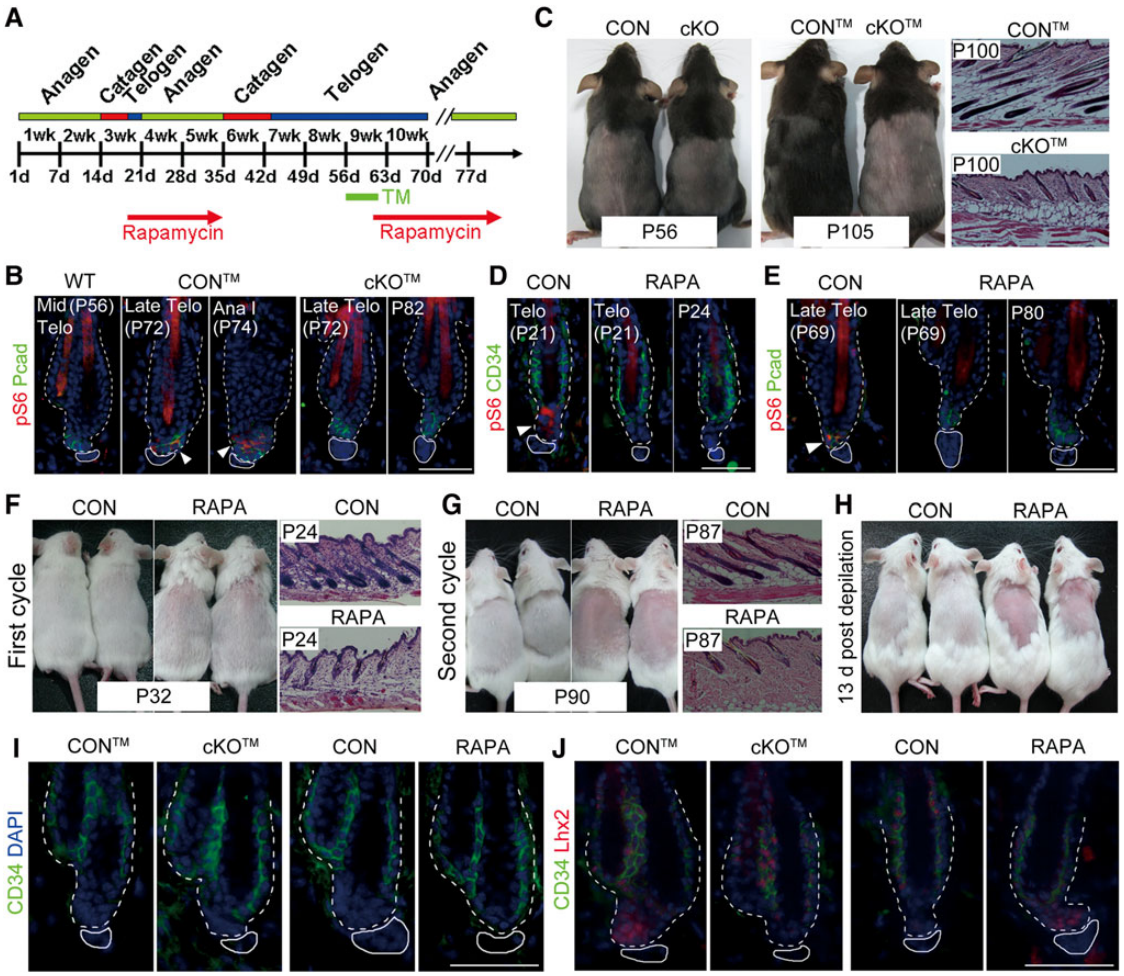

Figure 2 Mice deficient in mTOR signaling show a prominently prolonged telogen. (**A**) The schematic of the progression through the first and second postnatal hair cycles and the schedule for tamoxifen (TM) and rapamycin (RAPA) administration. (**B**) Verification that mTORC1 signaling is deleted in HFs of cKO^{TM} mice by pS6 immunostaining. Arrowheads indicate cells that express pS6. (**C**) Phenotypes of CON^{TM} and cKO^{TM} mice whose mTOR signaling was deleted in epidermis before anagen initiation. The hair coats of mice were clipped at second mid-telogen (P56). Note that hair coat recovery in CON^{TM} mice ($n = 10$, n stands for mouse number) was almost completed by P105, but cKO^{TM}-matched littermates ($n = 9$) still had little or no signs of recovery. H&E-stained skin sections on P100 demonstrated that HFs deficient in mTOR signaling showed extended telogen. (**D** and **E**) Validation that mTORC1 signaling is inhibited in RAPA HFs by pS6 immunostaining. Arrowheads note pS6-expressing cells. (**F** and **G**) Phenotypes of CON and RAPA mice whose mTOR signaling was inhibited before anagen onset. The hair coats of mice were clipped respectively at first telogen (P19) and at second mid-telogen (P56) according to the experimental needs. Note that hair coat recovery in CON mice ($n = 15$) was almost completed by P32/P90, but RAPA-matched littermates ($n = 12$) still had little or no signs of recovery. H&E-stained skin sections at P24/P87 demonstrated that HFs lacking mTOR signaling showed prolonged telogen. (**H**) Phenotypes of depilated mice treated with vehicle (CON) ($n = 15$) or rapamycin (RAPA) ($n = 15$). (**I** and **J**) Immunostaining of bulge-specific CD34 and bulge/HG marker Lhx2 in telogen HFs. Scale bar, 50 μm.

The body maturation was delayed in mice treated with RAPA in the first hair cycle (Supplementary Figure S2C). However, there was no statistically significant difference between CON and RAPA mice in the second hair cycle (Supplementary Figure S2D and E), indicating that the delay of anagen entry in RAPA mice does not result from the delay of entire body maturation. As expected, mice depilated in mid-telogen treated with RAPA (even with topical application of RAPA) displayed evidently delayed hair growth (Figure 2H and Supplementary Figure S2F). Moreover, depilated mice treated with another mTOR inhibitor, Torin 1 (Francipane and Lagasse, 2013), also showed a significant delay in hair regrowth (Supplementary Figure S2G).

In the extended second telogen, the hair regrowth was significantly delayed in mTOR signaling-deficient mice whose hair coat recovery appeared ~1 month later than normal (Supplementary Figure S2H and I). In spite of this delay, the HF morphologies and established markers were normal (Figure 2I and J).

Stem cell activation is delayed in hair follicles deficient in mTOR signaling

The mTOR/pS6 signaling pattern upon anagen initiation paralleled the two-step HFSC activation as previously reported (Greco et al., 2009), together with the phenotype that cKO^{TM}/RAPA HFs

exhibited significantly prolonged telogen, suggesting that stem cell activation in hair follicles might be delayed when mTOR signaling was lost. To figure out whether mTOR signaling functions in the activation of HFSCs, we analyzed the proliferative activity of HFs by immunostaining skin sections for the proliferative markers, Ki67 and BrdU. Ki67^{+} or BrdU^{+} nuclei had already occurred in HG cells adjacent to the DP at late telogen, which spread in most HG cells (also in HFSCs at the bulge base) as follicles began cycling in CON^{TM} mice, while cKO^{TM} HG cells displayed little or no Ki67 or BrdU staining even 10 days after late telogen (Figure 3A and Supplementary Figure S3A).

The same results were obtained from mice treated with RAPA before anagen onset in both the first and second hair cycles (Figure 3B, D and Supplementary Figure S3B). Particularly, at P22, CON HFs had already reached the first anagen and showed Ki67^{+} HG cells, while RAPA HFs were still in telogen (Figure 3C). Moreover, HFSC activation was also delayed evidently in depilated mice treated with RAPA or Torin 1 (Figure 3E and Supplementary Figure S3C), further conforming that mTOR signaling is required for HFSC activation.

Thus, the delayed stem cell activation appeared to be responsible for the deferred hair regeneration in mTOR signaling-deficient

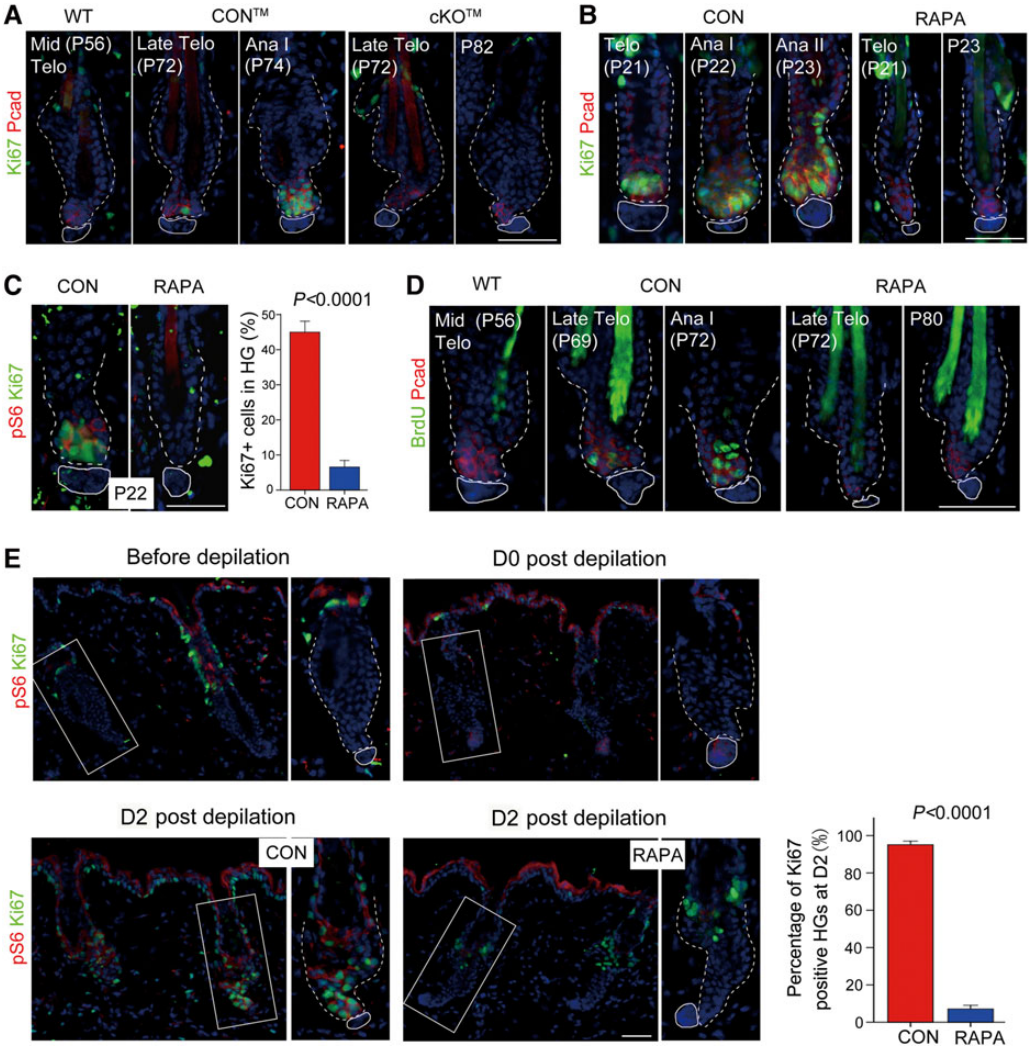

Figure 3 Hair follicles deficient in mTOR signaling display a delay in HFSC activation. (**A**–**D**) HFSC activation is delayed in mTOR signaling-deficient mice. (**A**) Immunostaining of the proliferative marker Ki67 in second mid-telogen (P56) WT HFs, second late telogen (P72) and anagen I (P76) CON^{TM} HFs, and second late telogen (P72) and P82 cKO^{TM} HFs. Note that nuclear Ki67 occurs in HFSCs in second late telogen CON^{TM} HFs, but not cKO^{TM} HFs (even by P82). (**B**) Ki67 immunostaining in telogen (P21), anagen I (P22), and P23 CON and RAPA HFs. (**C**) Immunolocalization of Ki67 and pS6 in CON and RAPA mice on P22. Quantification of Ki67^{+} HG cells ($n = 4$, >100 HG cells in each mouse) shown at right. (**D**) Immunostaining of BrdU in second mid-telogen (P56) WT HFs, second late telogen (P69) and anagen I (P74) CON HFs, and second late telogen (P72) and P80 RAPA HFs. Note that nuclear BrdU occurs in HFSCs in second late telogen CON HFs, but not RAPA HFs (even by P80). (**E**) Immunolocalization of Ki67 and pS6 in HFs of depilated mice treated with vehicle (CON) or rapamycin (RAPA) before depilation (P56), 0 day (D0) post depilation, and 2 days (D2) post depilation. Right panels, magnified images of boxed areas. Quantification of Ki67^{+} HGs ($n = 5$, >50 HGs in each mouse) shown at right. Data are reported as mean $\pm$ SEM. *P*-values were calculated using the Student's *t*-test. Scale bar, 50 μm.

mice. Based on these data presented so far, we also suggested that HFSCs of mTOR signaling-deficient mice were eventually activated once they received sufficient activating cues; then HFs entered what seemed to be an otherwise normal hair follicle cycle.

BMP signaling is consistently activated in hair follicle stem cells when mTOR signaling is lost

At the telogen-to-anagen transition, HFSCs must overcome high BMP signaling that maintains them in a quiescent state in order to initiate hair regeneration (Zhang et al., 2006; Kobielak et al., 2007; Plikus et al., 2008; Oshimori and Fuchs, 2012). The activation of mTOR signaling in DP and HFSCs happens to coincide with the timing when BMP signaling declines. Given that mTOR and BMP signaling seemed to have opposite effects on the activation of HFSCs, we examined whether mTOR signaling affected BMP pathway.

First, we assessed the effects of losing mTOR signaling on BMP signaling in HFSCs. Our data showed that nuclear phospho-Smad1/5/8 (pSmad1/5/8), an indication of active BMP signaling (Sapkota et al., 2007), was detected throughout the early and mid-telogen, but began to fade at the end of telogen, which was consistent with the occurrence of pS6 (Figures 4A, B and 1B). However, pSmad1/5/8 levels remained high in mTOR signaling-deficient HFSCs throughout this period (Figure 4A and B). Similarly, nuclear pSmad1/5/8 still remained high in HFSCs of depilated mice treated with RAPA while it waned in CON HFSCs 2 days post depilation (Figure 4C). These results suggest that BMP signaling is prolonged when HFSCs cannot sense mTOR signaling, which gives us a hint that mTOR signaling appears to have a negative effect on BMP signaling in HFSC activation.

To further explore the effects of mTOR signaling on HFSCs, we examined the antiproliferative effects of pharmacological inhibition of mTOR by rapamycin in a dose-dependent manner (0–100 nM) in bulge cells (HFSCs) *in vitro*. Our results showed that rapamycin significantly suppressed the proliferation of bulge cells even at a low dose (1 nM) (Figure 5A). Given this, the following pharmacological inhibition of mTOR *in vitro* was all achieved with 10 nM rapamycin (Supplementary Figure S4A). Similarly, after treated with rapamycin for 24 h, bulge cells showed defects in cell proliferation (75% reduction of BrdU incorporation) (Figure 5B).

Consistent with the observation that BMP signaling was extended when HFSCs cannot respond to mTOR signaling *in vivo* (Figure 4A–C), inhibition of mTORC1 by rapamycin resulted in increased levels of Smad1/5/8 phosphorylation that could be obviously relieved by Noggin, a potent BMP antagonist (Plikus et al., 2008; Oshimori and

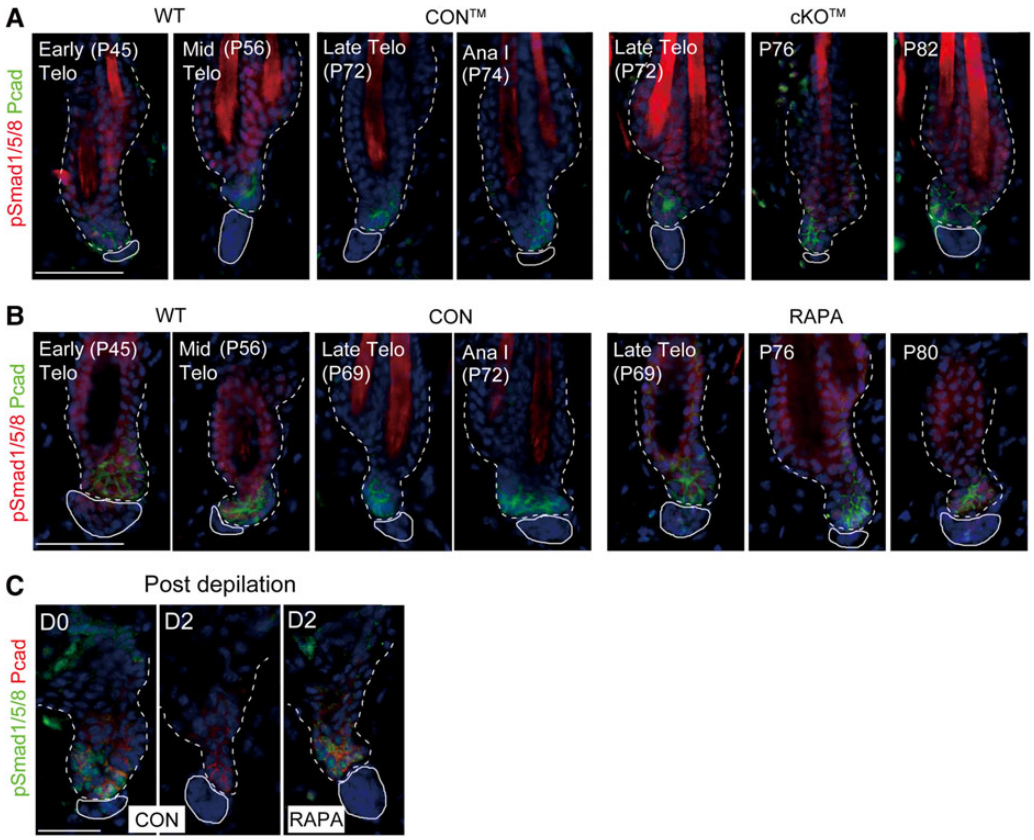

Figure 4 BMP signaling is prolonged in HFs deficient in mTOR signaling. (**A** and **B**) Immunolocalization of pSmad1/5/8 in second early telogen (P45), second mid -telogen (P56) WT HFs, second late telogen (P72/P69) and anagen I CON^{TM}/CON HFs, and second late telogen (P72/P69), P76, and P82/P80 cKO^{TM}/RAPA HFs. Note that nuclear pSmad1/5/8 (active BMP signaling) begins to wane in second late telogen CON^{TM}/CON HFs but not cKO^{TM}/RAPA HFs. (**C**) Immunolocalization of pSmad1/5/8 in HFs of depilated mice treated with vehicle (CON) or rapamycin (RAPA) 0 day (D0) and 2 days (D2) post depilation. Scale bar, 50 μm.

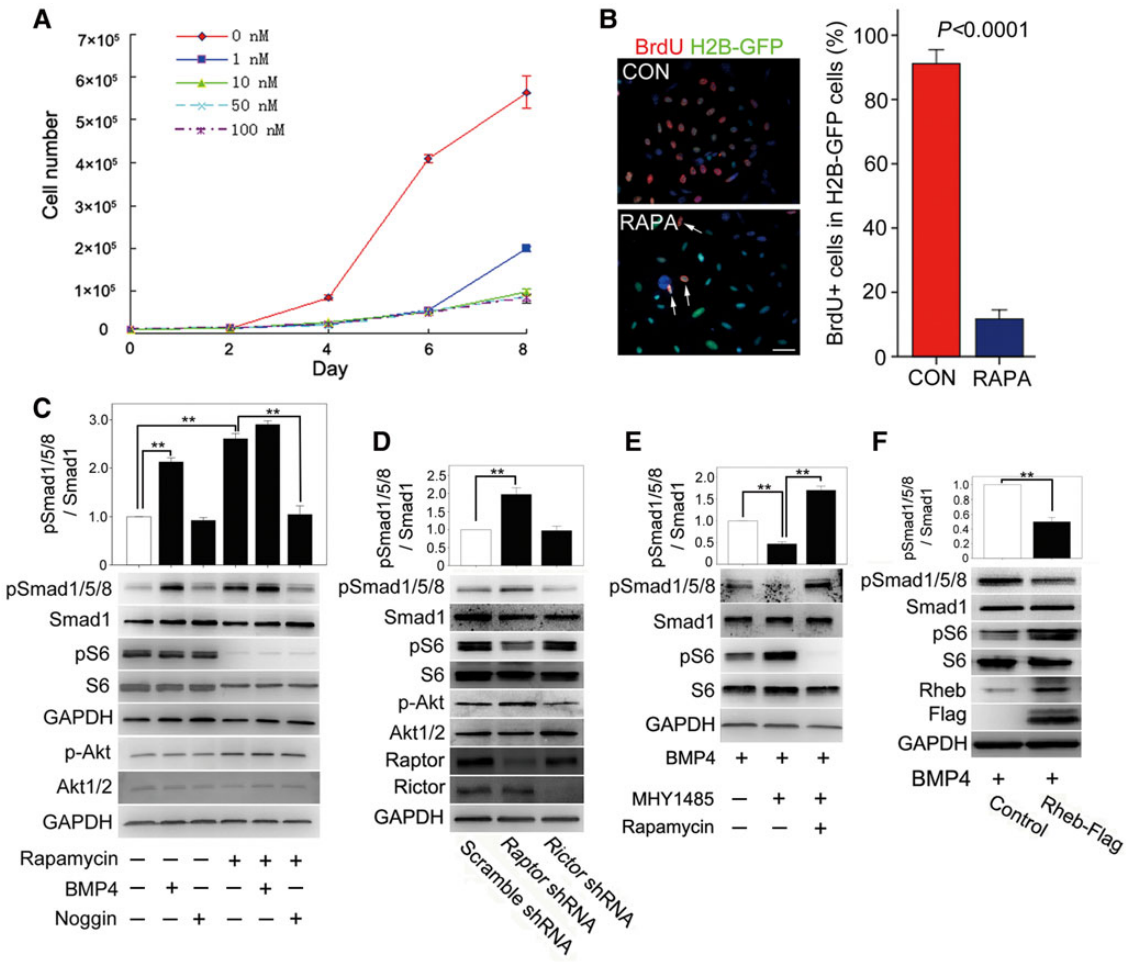

Figure 5 mTORC1 signaling negatively regulates BMP signaling in HFSCs. (**A**) Bulge cells (1×10^4 cells) were plated in 24-well dishes and cultured in the presence of different concentrations of rapamycin (0–100 nM) for 8 days. Growth curves indicate the mean of three independent experiments (± SEM). (**B**) BrdU incorporation in H2B-GFP bulge cells treated with 10 nM rapamycin for 24 h. Quantification of BrdU incorporation in vehicle (CON) and rapamycin (RAPA) groups shown at right. *P*-value was calculated using the Student's *t*-test. Scale bar, 50 μm. (**C**) Immunoblotting analysis of cell lysates from bulge cells stimulated with BMP4 or Noggin in the presence or absence of rapamycin for 24 h. (**D**) Immunoblotting of cell lysates from scrambled, *Raptor*, or *Rictor* shRNA-transduced bulge cells. (**E**) Immunoblotting analysis of cell lysates from bulge cells treated with BMP4 and stimulated with MHY1485, alone or with rapamycin, for 24 h. (**F**) Immunoblotting analysis of cell lysates from control and Rheb-Flag-overexpressing bulge cells treated with BMP4. The typical blot was presented and quantification of three independent experiments is shown for **C**–**F**. *Y*-axis represents relative intensity (measured with Image J) normalized to the signal of vehicle (Control, 100%). Data are reported as mean ± SEM. Student's *t*-test was used to compare data. ** $P < 0.01$.

Fuchs, 2012), in bulge cells *in vitro* (Figure 5C). In contrast, activation or inhibition of BMP signaling by BMP4 or Noggin had no effect on mTORC1 signaling (Figure 5C and Supplementary Figure S4B), indicating that mTOR signaling may act as an upstream regulator of BMP signaling. To further investigate whether mTOR signaling negatively affected BMP signaling, we performed lentiviral shRNA-mediated gene knockdown experiments to respectively knock down Raptor, an essential component of mTORC1, and Rictor, a subunit of mTORC2 (Russell et al., 2011; Laplante and Sabatini, 2012), in bulge cells. Immunoblot analysis showed that in cells transduced with *Raptor* shRNA, decreased mTORC1 activity resulted in elevated Smad1/5/8 phosphorylation. However, reduced activity of mTORC2 did not affect Smad1/5/8 phosphorylation in cells transduced with *Rictor* shRNA (Figure 5D). In contrast, activation of mTORC1 by MHY1485, an mTOR activator (Choi et al., 2012), caused an increase in the level of Smad1/5/8 phosphorylation, which could be reversed by rapamycin (Figure 5E). Also, introducing Flag-tagged Rheb, a GTPase upstream of mTORC1 (Russell et al., 2011), into BMP4-stimulated bulge cells resulted in strong suppression of Smad1/5/8 phosphorylation (Figure 5F). Moreover, we found that inhibition of mTOR signaling did not have an obvious impact on Wnt/β-catenin and TGF-β signaling, two other critical pathways involved in HFSC activation (Supplementary Figure S4C and D). Collectively, these data indicate that mTOR signaling negatively affects BMP signaling in HFSCs.

Exogenously delivered BMP antagonist Noggin can rescue the delayed HFSC activation in mTOR signaling-deficient mice

To test the hypothesis that mTOR signaling acts positively to overcome high levels of BMP signaling to activate HFSCs, we evaluated whether exogenously delivered BMP antagonist Noggin could rescue the delayed HFSC activation and extended telogen in mTOR signaling-deficient mice. At the end of second telogen, we intradermally injected cKO^{TM} or RAPA mice with Noggin or BSA together with fluorescent beads for 4 consecutive days (Supplementary Figure S5A). Within 3 days, nuclear pSmad1/5/8 waned in HFs of cKO^{TM} or RAPA mice injected with Noggin (Supplementary Figure S5B). By Ki67 and BrdU immunostaining, we showed that the proliferation of HFSCs near the Noggin rather than BSA beads injection site had been greatly restored in cKO^{TM} and RAPA mice (Figure 6A, C, and Supplementary Figure S5C and D). Furthermore, 3 weeks after injection, the delayed hair regrowth was rescued at the injection site of Noggin beads in both cKO^{TM} and RAPA mice (Figure 6B and D).

Taken together, these findings demonstrate that mTOR signaling regulates HFSC activation at least partially through counterbalancing BMP-mediated suppression during hair regeneration.

Discussion

The data presented here show that mTORC1 signaling is critical for the activation of hair follicle stem cells during hair regeneration. By using both genetic and pharmacological approaches, we show that loss of mTOR signaling before anagen onset in adult skin epithelial cells leads to delayed HFSC activation, and consequently results in significantly extended telogen.

Recently, it was discovered that inhibition of mTOR signaling by systemic application of rapamycin, the specific mTORC1 inhibitor, resulted in delayed hair cycle initiation in the first hair cycle (Kellenberger and Tauchi, 2013). Our findings now demonstrate that, by employing both an inducible conditional gene targeting strategy and a pharmacological inhibition method to delete or inhibit mTOR signaling in adult skin epithelium before anagen initiation, HFs that cannot sense mTOR signaling exhibit significantly delayed HFSC activation and extended telogen. Further, we identify that mTORC1 signaling plays an essential role in promoting stem cell activation through counterbalancing BMP-mediated repression upon anagen initiation. Although depilation has been shown to immediately induce homogeneous anagen entry over the whole depilated back skin of the mouse by using wax/rosin mixture (Muller-Rover et al., 2001), the potential mechanism of anagen induction remains unclear. Our results now show that, after depilation, mTORC1 signaling is soon activated in HFSCs, and inhibition of this signaling leads to delayed anagen initiation, indicating that mTORC1 signaling may also govern the anagen entry in depilation-induced hair follicle cycling. Interestingly, Stat3, an mTOR downstream molecule, has been shown to mediate spontaneous anagen entry but not pluck-induced anagen (Sano et al., 1999, 2000). Our data now show that mTOR control both spontaneous anagen initiation and depilation-induced hair cycling. Therefore, we suggest that there are multiple downstream signals of mTOR, which separately control spontaneous anagen entry and pluck-induced anagen, and Stat3 is one of the downstream signals of mTOR that controls spontaneous anagen entry.

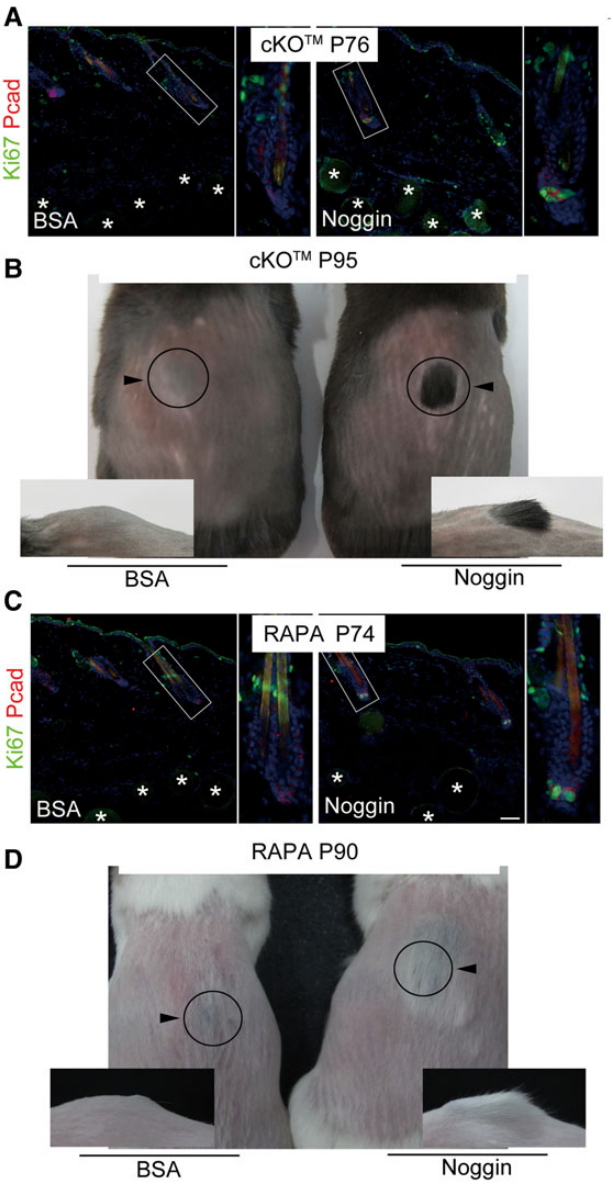

Figure 6 Exogenously supplied BMP antagonist Noggin can ameliorate the delayed HFSC activation in mTOR signaling-deficient mice. (**A** and **C**) Immunostaining of Ki67 in HFs of cKO^{TM} (**A**) or RAPA (**C**) mice intradermally injected with BSA or Noggin beads. Right panels, magnified views of boxed areas. Asterisks note the injected beads soaked with BSA or Noggin. (**B** and **D**) Hair coats of cKO^{TM} (**B**) ($n = 6$) or RAPA (**D**) ($n = 7$) mice were clipped, and mice were intradermally injected with BSA or Noggin beads at the indicated time. Hair growth was monitored on P95 or P90 at the injection sites (solid black circles). Amplified views of these areas are shown on either side. Note ameliorative hair growth at Noggin injection site. Scale bar, 50 μm.

At the beginning of telogen, extrinsic and intrinsic BMP signaling is high, but then gradually declines in HFSCs at late telogen. In contrast, BMP inhibitors generated by the surrounding niche rise over telogen, thereby lowering the threshold of BMP signaling that

maintains HFSCs quiescence to launch hair growth (Plikus et al., 2008; Oshimori and Fuchs, 2012). Our data here reveal an essential role for mTOR signaling in facilitating HFSC activation via counterbalancing the suppressive effects of BMP signaling during hair regeneration. Considering that mTOR pathway senses and integrates a series of environmental cues, especially nutrient availability and energy status, to regulate tissue growth and homeostasis (Russell et al., 2011; Laplante and Sabatini, 2012), we propose that hair follicles may integrate a variety of nutrient and energy signals from the surrounding environment to get over the suppressive cues, such as BMP signaling, to promote hair growth.

It has been shown that BMP cycle occurs out of phase with the Wnt/β-catenin cycle, thus dividing the conventional telogen into two functional phases: one refractory and the other competent for hair regeneration, characterized by high and low BMP signaling, respectively (Plikus et al., 2008). Moreover, the cross talk between BMP signaling and other signals, such as Wnt and TGFβs, at the competent telogen plays an essential role in HFSC activation (Oshimori and Fuchs, 2012; Plikus, 2012; Kandyba et al., 2013). Our findings now show that the activation of mTOR signaling is out of phase with BMP signaling during the telogen-to-anagen transition and promotes stem cell activation through counterbalancing BMP-mediated suppression, adding new evidence for cross talk between the BMP- and mTOR-activating signaling pathways at the competent telogen that is responsible for hair regeneration.

Although HFs deficient in mTOR signaling exhibit an unusually extended telogen phase, they eventually overcome the high level of BMP signaling and enter into the next hair cycle. These findings indicate that mTOR signaling functions specifically in the HFSC activation, and the regulation of HFSC activation does not rely on a single factor or a certain cell type but rather delicately responds to the global environment surrounding the HFSCs. By both genetic and pharmacological evidences, we identify that mTOR signaling functions as an important member of the complicated signaling networks involved in hair regeneration.

At the end of telogen, HG cells begin to proliferate and generate transit-amplifying cells (TACs) to initiate HF regeneration in response to DP signals (Greco et al., 2009; Enshell-Seijffers et al., 2010; Kandyba et al., 2013; Hsu et al., 2014). The activation of mTOR signaling was not observed in DP at the onset of anagen in spontaneous hair cycle, possibly due to that it may last for only a short period of time. Intriguingly, we detected strong signs of active mTOR signaling in DP just few hours after depilation, and as HFs began cycling, the active signs waned in DP and appeared in HFSCs (Figure 1E and F). This fascinating finding strongly suggests that DP is the first major source of mTOR signaling activated transiently at the telogen-to-anagen transition; then anagen begins when mTOR signaling is activated in HFSCs responding to DP signals.

Consistent with a role for mTOR signaling in regulating the proliferation of stem cells (Javier et al., 1997; Murakami et al., 2004; Ryu and Han, 2011), we found that inhibition of mTOR signaling blocks the proliferation of HFSCs. In addition, based on our genetic evidences, together with the pharmacological results, we uncover that mTOR signaling acts as a crucial regulator in governing the balance between HFSC quiescence and activation during hair regeneration, which coincides with previous studies in other tissues. For instance, mTOR signaling is pivotal in determining proliferation versus quiescence in the adult forebrain neural stem cell niche (Paliouras et al., 2012). Similarly, mTOR signaling plays a role in regulating hematopoietic stem cell quiescence (Chen et al., 2008; Gan and DePinho, 2009).

BMP signaling acts as a negative role in the proliferation of stem cells in some niches including the bulge (Haramis et al., 2004; Plikus et al., 2008). It seems to be a crucial step to restrain BMP signaling in facilitating stem cell activation during tissue regeneration. Our findings uncover a role for mTOR signaling in repressing BMP signaling, which adds new insights into the stem cell activation. Although our study shows that mTOR signaling appears to negatively regulate BMP signaling, we anticipate that mTOR/pS6 signaling plays an indirect role in the phosphorylation events of Smad1/5/8 rather than regulating BMP signaling directly, and the accurate cross talk between the two signaling requires further study.

In conclusion, we have shown that mTOR signaling plays a key role in promoting stem cell activation at least partially through counterbalancing BMP-mediated suppression during hair regeneration. Currently, we are undertaking further studies to figure out the precise mechanism by which mTOR/pS6 pathway regulates BMP signaling.

Materials and methods

Mice, rapamycin treatment, and BrdU labeling

mTOR-floxed mice (Risson et al., 2009) were crossed with *K14-CreER* mice (Vasioukhin et al., 1999), and targeting was achieved by intraperitoneal injection of TM (150 μg/g mice, Sigma-Aldrich) (Hsu et al., 2011) for 5 days. For rapamycin administration, CD1 mice (Vital River Laboratories, Beijing, China) were administered with rapamycin (LC Laboratories) through intraperitoneal injection at a dose of 4 mg/kg per day (Castilho et al., 2009) at the indicated time before analyses. Before treated with tamoxifen or rapamycin, the back skins of mice (all mice used in this study were sex-matched) were shaved at P56, corresponding to the middle stage of the second postnatal telogen. For 5-Bromo-2′-deoxyuridine (BrdU) pulse experiments, mice were injected intraperitoneally with 50 μg/g BrdU (Sigma-Aldrich) prior to being sacrificed. All mice were maintained under specified-pathogen-free (SPF) conditions and procedures performed were in accordance with instructions and permissions of the ethical committee of the Institute of Zoology, Chinese Academy of Sciences.

Skin harvest, histology, and immunofluorescence

Back skins were harvested from the mid-dorsal areas. Distinct hair cycle stages were judged as previously described (Muller-Rover et al., 2001; Greco et al., 2009; Oshimori and Fuchs, 2012). Hematoxylin and Eosin (H&E) staining and immunofluorescence were performed as previously described (Nguyen et al., 2006; Hu et al., 2012; Oshimori and Fuchs, 2012). Back skins from mice were embedded and frozen in OCT (Tissue Tek). Frozen back skin sections (8–10 μm) were fixed for 10 min with paraformaldehyde (PFA), washed with phosphate-buffered saline (PBS), and then blocked for 1 h in blocking buffer (5% NGS, 1% BSA, 0.3% Triton X-100) or blocks (5% NDS, 1% BSA, 0.3% Triton X-100). For BrdU

immunofluorescence, sections were pretreated with 1 N HCl for 1 h at 37°C before blocked. Primary antibodies were incubated at 4°C overnight. After washing with PBS, FITC- or TRITC-conjugated secondary antibody (Santa Cruz Biotechnology) was added for 1 h at room temperature. Sections were washed and counterstained with 4′,6-diamidino-2-phenylindole (DAPI). All images were acquired with a Zeiss Axioplan 2 microscope. The following primary antibodies were used: rabbit anti-phospho-S6 ribosomal protein (Ser235/236) (pS6) (1:200, Cell Signaling Technology), rabbit anti-mTOR (1:200, Cell Signaling Technology), rabbit anti-phospho-Akt (Ser473) (1:200, Cell Signaling Technology), rat anti-CD34 (1:400, eBioscience), rat anti-P-cadherin (1:100, R&D Systems), goat anti-P-cadherin (1:100, R&D Systems), rabbit anti-Ki67 (1:500, Abcam), rat anti-Ki67 (1:500, eBioscience), goat anti-Lhx2 (1:200, Santa Cruz Biotechnology), rat anti-BrdU (1:200, Abcam), and rabbit anti-pSmad1/5/8 (Ser463/465) (1:500, Millipore).

Fluorescence activated cell sorting

Bulge cells from different stages of hair cycle were isolated by fluorescence activated cell sorting (FACS) using the surface markers α6-integrin (CD49f) and CD34 as described previously (Blanpain et al., 2004). DAPI was used to eliminate the dead cells. Sorted cells were used for protein preparation for immunoblotting.

Cell culture

Mouse H2B-GFP bulge cells were cocultured with NIH 3T3 feeder cells as described (Oshimori and Fuchs, 2012). For stimulation experiments, we added media including rapamycin (10 nM, LC Laboratories), human BMP4 (1 nM, R&D Systems), or mouse Noggin (500 ng/ml, R&D Systems), and cultured for 24 h. For MHY1485 stimulation experiments, after starved overnight, bulge cells were stimulated with medium containing BMP4 and MHY1485 (2 μM, Sigma) for 24 h. For overexpression experiments, PRK-Flag-Rheb and pCDNA 3.0 plasmids, generous gifts from Jie Chen laboratory (Ge et al., 2011), were transfected into bulge cells by using Fugene HD transfection reagent (Promega) following the manufacturer's recommendations, and then bulge cells were stimulated with human BMP4 (1 nM, R&D Systems) for 24 h after starved overnight. Bulge cells were then harvested, and proteins were extracted for immunoblotting analysis.

Lentivirus-mediated RNAi

Lentiviral constructs that encode shRNAs against mouse Raptor and Rictor were kind gifts from Jie Chen laboratory (Ge et al., 2011). The lentiviruses were produced in 293T cells. For viral infections, bulge cells were incubated with lentivirus in the presence of polybrene (80 μg/ml). Bulge cells were then harvested, and proteins were extracted for immunoblotting analysis.

Immunoblotting

Proteins were prepared by using RAPA lysis buffer (Beyotime) according to the manufacturer's instruction. Protein lysates were mixed with 5× SDS sample buffer, and heated at 95°C for 5 min. For immunoblotting, proteins were resolved by SDS–PAGE and transferred onto PVDF membranes (Millipore). After blocked, the PVDF membranes containing proteins were incubated with primary antibodies diluted in blocking buffer. The final detection was performed by using a horseradish (HRP)-conjugated secondary antibody (Santa Cruz Biotechnology). Primary antibodies used were: rabbit anti-phospho-S6 ribosomal protein (Ser235/236) (pS6) (1:2000, Cell Signaling Technology), rabbit anti-S6 ribosomal protein (S6) (1:2000, Cell Signaling Technology), rabbit anti-phospho-Akt (Ser473) (1:1000, Cell Signaling Technology), goat anti-Akt1/2 (1:1000, Santa Cruz Biotechnology), rabbit anti-pSmad1/5/8 (Ser463/465) (1:3000, Millipore), rabbit anti-Smad1 (1:1000, Cell Signaling Technology), rabbit anti-Raptor (1:1000, Cell Signaling Technology), rabbit anti-Rictor (1:1000, Cell Signaling Technology), mouse anti-Flag (1:5000, Cell Signaling Technology), mouse anti-Rheb (1:1000, R&D Systems), and mouse anti-GAPDH (1:5000, Cell Signaling Technology).

Protein beads injection

Mice were intradermally injected with recombinant mouse Noggin (200 ng/mouse, R&D Systems) or 0.1% BSA together with beads for 4 days as previously described (Chen et al., 2012). The skins were harvested and analyzed at the indicated time.

Statistical analysis

Statistical analysis was performed using SPSS and Microsoft Excel. Data were analyzed by using unpaired two-tailed Student's *t*-test. Significant differences between two groups were noted by actual *P*-values.

Supplementary material

Supplementary material is available at *Journal of Molecular Cell Biology* online.

Acknowledgements

We thank Elaine Fuchs (Rockefeller University, New York, USA) for the mouse H2B-GFP bulge cell line and Jie Chen (University of Illinois at Urbana-Champaign, USA) for *Raptor* and *Rictor* shRNAs, and Flag-Rheb plasmid. We thank Aaron JW Hsueh (Stanford University, USA) and Dong Li (University of Illinois at Urbana-Champaign, USA) for their thoughtful discussions throughout this work.

Funding

This work was supported by grants from the Strategic Priority Research Program of the Chinese Academy of Sciences (XDA 01010202 to E.D. and XDA 04020202-20), the National Basic Research Program of China (2011CB710905 to E.D.), and the National Natural Science Foundation of China (31201099 to S.L. and 31471287 to E.D.).

Conflict of interest: none declared.

References

Andl, T., Reddy, S.T., Gaddapara, T., et al. (2002). WNT signals are required for the initiation of hair follicle development. Dev. Cell *2*, 643–653.

Blanpain, C., Lowry, W.E., Geoghegan, A., et al. (2004). Self-renewal, multipotency, and the existence of two cell populations within an epithelial stem cell niche. Cell *118*, 635–648.

Botchkarev, V.A., Botchkareva, N.V., Nakamura, M., et al. (2001). Noggin is required for induction of the hair follicle growth phase in postnatal skin. FASEB J. *15*, 2205–2214.

Castilho, R.M., Squarize, C.H., Chodosh, L.A., et al. (2009). mTOR mediates Wnt-induced epidermal stem cell exhaustion and aging. Cell Stem Cell *5*, 279–289.

Chen, C., Liu, Y., Liu, R., et al. (2008). TSC-mTOR maintains quiescence and function of hematopoietic stem cells by repressing mitochondrial biogenesis and reactive oxygen species. J. Exp. Med. *205*, 2397–2408.

Chen, T., Heller, E., Beronja, S., et al. (2012). An RNA interference screen uncovers a new molecule in stem cell self-renewal and long-term regeneration. Nature *485*, 104–108.

Choi, Y.J., Park, Y.J., Park, J.Y., et al. (2012). Inhibitory effect of mTOR activator MHY1485 on autophagy: suppression of lysosomal fusion. PLoS One *7*, e43418.

Cotsarelis, G., Sun, T.T., and Lavker, R.M. (1990). Label-retaining cells reside in the bulge area of pilosebaceous unit: implications for follicular stem cells, hair cycle, and skin carcinogenesis. Cell *61*, 1329–1337.

Enshell-Seijffers, D., Lindon, C., Kashiwagi, M., et al. (2010). beta-catenin activity in the dermal papilla regulates morphogenesis and regeneration of hair. Dev. Cell *18*, 633–642.

Francipane, M.G., and Lagasse, E. (2013). Selective targeting of human colon cancer stem-like cells by the mTOR inhibitor Torin-1. Oncotarget *4*, 1948–1962.

Gan, B., and DePinho, R.A. (2009). mTORC1 signaling governs hematopoietic stem cell quiescence. Cell Cycle *8*, 1003–1006.

Gan, B., Hu, J., Jiang, S., et al. (2010). Lkb1 regulates quiescence and metabolic homeostasis of haematopoietic stem cells. Nature *468*, 701–704.

Ge, Y., Yoon, M.S., and Chen, J. (2011). Raptor and Rheb negatively regulate skeletal myogenesis through suppression of insulin receptor substrate 1 (IRS1). J. Biol. Chem. *286*, 35675–35682.

Greco, V., Chen, T., Rendl, M., et al. (2009). A two-step mechanism for stem cell activation during hair regeneration. Cell Stem Cell *4*, 155–169.

Haramis, A.P., Begthel, H., van den Born, M., et al. (2004). De novo crypt formation and juvenile polyposis on BMP inhibition in mouse intestine. Science *303*, 1684–1686.

Hay, N., and Sonenberg, N. (2004). Upstream and downstream of mTOR. Genes Dev. *18*, 1926–1945.

Horsley, V., Aliprantis, A.O., Polak, L., et al. (2008). NFATc1 balances quiescence and proliferation of skin stem cells. Cell *132*, 299–310.

Hsu, Y.C., Pasolli, H.A., and Fuchs, E. (2011). Dynamics between stem cells, niche, and progeny in the hair follicle. Cell *144*, 92–105.

Hsu, Y.C., Li, L., and Fuchs, E. (2014). Transit-amplifying cells orchestrate stem cell activity and tissue regeneration. Cell *157*, 935–949.

Hu, H.M., Zhang, S.B., Lei, X.H., et al. (2012). Estrogen leads to reversible hair cycle retardation through inducing premature catagen and maintaining telogen. PLoS One *7*, e40124.

Javier, A.F., Bata-Csorgo, Z., Ellis, C.N., et al. (1997). Rapamycin (sirolimus) inhibits proliferating cell nuclear antigen expression and blocks cell cycle in the G1 phase in human keratinocyte stem cells. J. Clin. Invest. *99*, 2094–2099.

Kandyba, E., Leung, Y., Chen, Y.B., et al. (2013). Competitive balance of intrabulge BMP/Wnt signaling reveals a robust gene network ruling stem cell homeostasis and cyclic activation. Proc. Natl Acad. Sci. USA *110*, 1351–1356.

Kellenberger, A.J., and Tauchi, M. (2013). Mammalian target of rapamycin complex 1 (mTORC1) may modulate the timing of anagen entry in mouse hair follicles. Exp. Dermatol. *22*, 77–80.

Kobielak, K., Stokes, N., de la Cruz, J., et al. (2007). Loss of a quiescent niche but not follicle stem cells in the absence of bone morphogenetic protein signaling. Proc. Natl Acad. Sci. USA *104*, 10063–10068.

Laplante, M., and Sabatini, D.M. (2012). mTOR signaling in growth control and disease. Cell *149*, 274–293.

Lowry, W.E., Blanpain, C., Nowak, J.A., et al. (2005). Defining the impact of beta-catenin/Tcf transactivation on epithelial stem cells. Genes Dev. *19*, 1596–1611.

Millar, S.E. (2002). Molecular mechanisms regulating hair follicle development. J. Invest. Dermatol. *118*, 216–225.

Muller-Rover, S., Handjiski, B., van der Veen, C., et al. (2001). A comprehensive guide for the accurate classification of murine hair follicles in distinct hair cycle stages. J. Invest. Dermatol. *117*, 3–15.

Murakami, M., Ichisaka, T., Maeda, M., et al. (2004). mTOR is essential for growth and proliferation in early mouse embryos and embryonic stem cells. Mol. Cell Biol. *24*, 6710–6718.

Nguyen, H., Rendl, M., and Fuchs, E. (2006). Tcf3 governs stem cell features and represses cell fate determination in skin. Cell *127*, 171–183.

Oshimori, N., and Fuchs, E. (2012). Paracrine TGF-beta signaling counterbalances BMP-mediated repression in hair follicle stem cell activation. Cell Stem Cell *10*, 63–75.

Paliouras, G.N., Hamilton, L.K., Aumont, A., et al. (2012). Mammalian target of rapamycin signaling is a key regulator of the transit-amplifying progenitor pool in the adult and aging forebrain. J. Neurosci. *32*, 15012–15026.

Plikus, M.V. (2012). New activators and inhibitors in the hair cycle clock: targeting stem cells' state of competence. J. Invest. Dermatol. *132*, 1321–1324.

Plikus, M.V., Mayer, J.A., de la Cruz, D., et al. (2008). Cyclic dermal BMP signalling regulates stem cell activation during hair regeneration. Nature *451*, 340–344.

Rabbani, P., Takeo, M., Chou, W., et al. (2011). Coordinated activation of Wnt in epithelial and melanocyte stem cells initiates pigmented hair regeneration. Cell *145*, 941–955.

Risson, V., Mazelin, L., Roceri, M., et al. (2009). Muscle inactivation of mTOR causes metabolic and dystrophin defects leading to severe myopathy. J. Cell Biol. *187*, 859–874.

Russell, R.C., Fang, C., and Guan, K.L. (2011). An emerging role for TOR signaling in mammalian tissue and stem cell physiology. Development *138*, 3343–3356.

Ryu, J.M., and Han, H.J. (2011). L-threonine regulates G1/S phase transition of mouse embryonic stem cells via PI3K/Akt, MAPKs, and mTORC pathways. J. Biol. Chem. *286*, 23667–23678.

Sano, S., Itami, S., Takeda, K., et al. (1999). Keratinocyte-specific ablation of Stat3 exhibits impaired skin remodeling, but does not affect skin morphogenesis. EMBO J. *18*, 4657–4668.

Sano, S., Kira, M., Takagi, S., et al. (2000). Two distinct signaling pathways in hair cycle induction: Stat3-dependent and -independent pathways. Proc. Natl Acad. Sci. USA *97*, 13824–13829.

Sapkota, G., Alarcon, C., Spagnoli, F.M., et al. (2007). Balancing BMP signaling through integrated inputs into the Smad1 linker. Mol. Cell *25*, 441–454.

Sarbassov, D.D., Guertin, D.A., Ali, S.M., et al. (2005). Phosphorylation and regulation of Akt/PKB by the rictor-mTOR complex. Science *307*, 1098–1101.

Schneider, M.R., Schmidt-Ullrich, R., and Paus, R. (2009). The hair follicle as a dynamic miniorgan. Curr. Biol. *19*, R132–R142.

Tumbar, T., Guasch, G., Greco, V., et al. (2004). Defining the epithelial stem cell niche in skin. Science *303*, 359–363.

Vasioukhin, V., Degenstein, L., Wise, B., et al. (1999). The magical touch: genome targeting in epidermal stem cells induced by tamoxifen application to mouse skin. Proc. Natl Acad. Sci. USA *96*, 8551–8556.

Wendel, H.G., De Stanchina, E., Fridman, J.S., et al. (2004). Survival signalling by Akt and eIF4E in oncogenesis and cancer therapy. Nature *428*, 332–337.

Zhang, J., He, X.C., Tong, W.G., et al. (2006). Bone morphogenetic protein signaling inhibits hair follicle anagen induction by restricting epithelial stem/progenitor cell activation and expansion. Stem Cells *24*, 2826–2839.

Zhang, Y., Andl, T., Yang, S.H., et al. (2008). Activation of beta-catenin signaling programs embryonic epidermis to hair follicle fate. Development *135*, 2161–2172.